Supplementary information

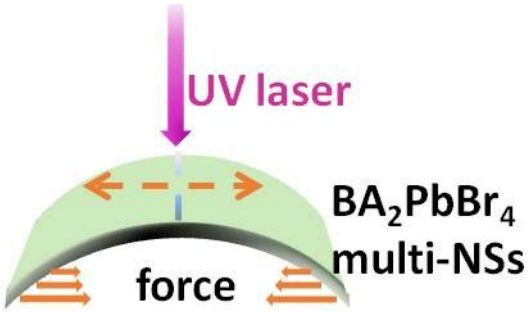

Figure S1. Schematic illustration of the tension over the BA_2PbBr_4 crystals.

Note I. Estimation of strain ε and tension σ

The strain of BA_2PbBr_4 was estimated according to the bending curvature, as shown in **Figure S2**. It is assumed that the strain variable of BA_2PbBr_4 is consistent with that of the PET substrate. Taking PET as the study object, the original length is l_0 (2 cm) and the thickness is d_0 (0.06 cm). When applying the tension along horizontal direction by bending PET, the upper surface of PET bears tensile stress and the bottom surface bears compressive stress. The upper and bottom surface produces tensile and compressive strain, respectively correspondingly. There should exist a curved neutral layer (marked in grey dotted line with the unchanged length l_0) without any strain.[1] Since all of the characterizations were focused on the center point of the upper surface, we calculated the strain generated on the upper surface by following approximation.

$$\varepsilon = \frac{\Delta l}{l_0} \approx \frac{\theta(r_0 + d_0/2) - l_0}{l_0} = \frac{0.03}{r_0} \quad (1)$$

where ε is the strain, Δl is the length variation, θ is the radian after bending, r_0 is the

radii of the curved neutral layer. The tension σ can be calculated out according to formula (2)

$$\sigma = \varepsilon E \tag{2}$$

where E is the elastic modulus (18.8 GPa). The corresponding θ, r_0, ε, σ used for above calculations are shown in **Table S1**.

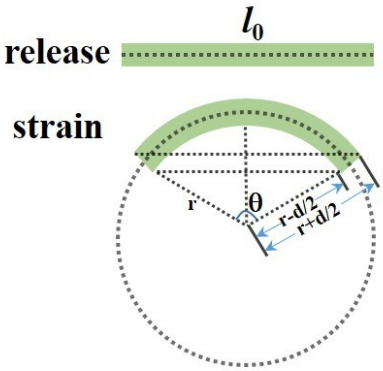

Figure S2. Schematic illustration of the shape change under strain, and the length was used for strain calculation in Figure S1.

Table S1. θ, r_0, ε, σ values for strain calculations.

θ (rad)	r_0 (cm)	ε (%)	σ (MPa)
0	+∞	0	0
0.07π	18.25	0.16	30
0.09π	14.29	0.21	40
0.11π	11.11	0.27	50
0.14π	9.38	0.32	60
0.17π	7.50	0.40	75
0.51π	2.50	1.20	225
1.08π	1.18	2.55	480

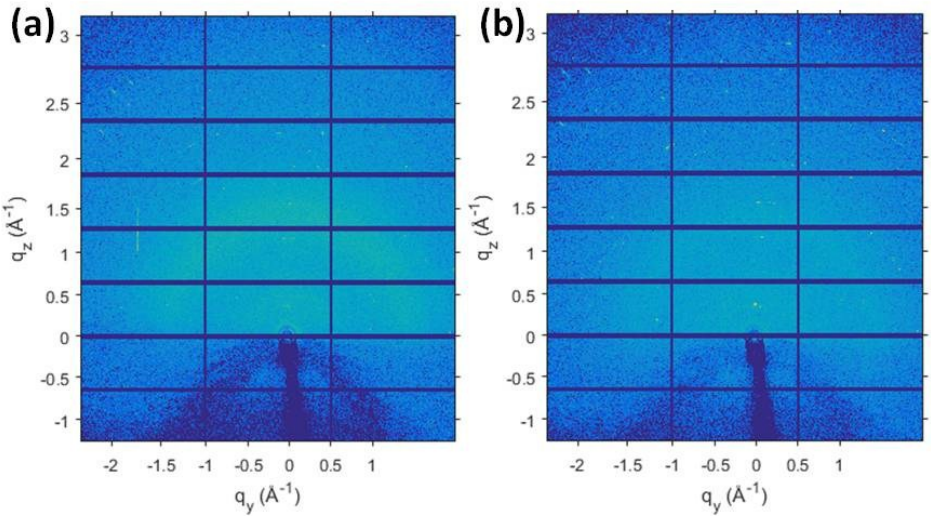

Figure S3. Grazing-incidence wide-angle X-ray scattering (GIWAXS) of BA_2PbBr_4 (a) without and (b) with tension

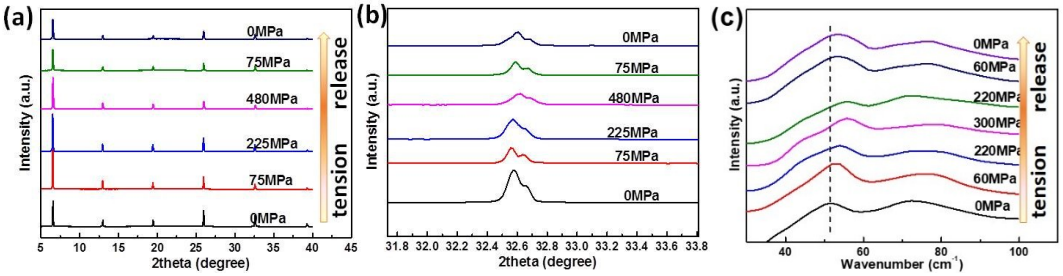

Figure S4. (a) X-ray patterns of BA_2PbBr_4 under different tensions, (b) the enlarged diffraction peak between 31^o and 34^o, (c) Raman spectra of BA_2PbBr_4 under different tensions by directly stretching horizontally

Table S2. The calculated lattice constant and tension of BA_2PbBr_4 under various tensile strains along *a/b* plane.

Lattice constant (Å)											
Strain	0%	0.5%	1.0%	1.5%	2.0%	2.5%	3.0%	3.5%	4.0%	4.5%	5.0%
a	8.253	8.305	8.346	8.387	8.429	8.470	8.511	8.553	8.594	8.635	8.677
b	8.137	8.189	8.230	8.271	8.311	8.352	8.393	8.434	8.474	8.515	8.556
c	27.403	27.120	27.014	26.932	26.822	26.731	26.602	26.516	26.499	26.390	26.293
Tension (MPa)											
Strain	0%	0.5%	1.0%	1.5%	2.0%	2.5%	3.0%	3.5%	4.0%	4.5%	5.0%
a/stress	0	293	399	523	638	749	831	890	990	1045	1061
b/stress	0	278	417	553	686	795	855	921	1009	1097	1142

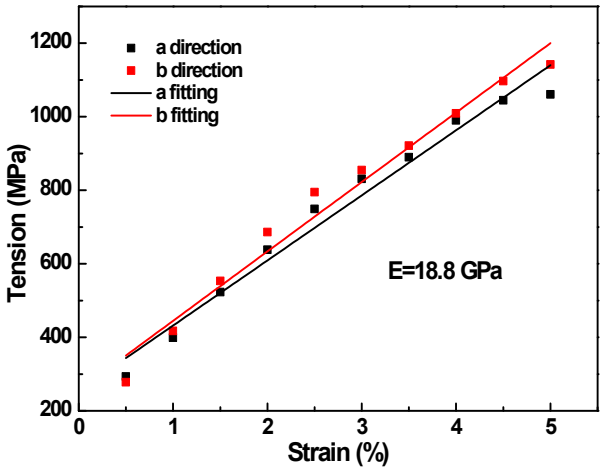

Figure S5. Calculation of Young's modulus of BA_2PbBr_4 along a/b directions by linearly fitting the calculated tension versus applied strain.

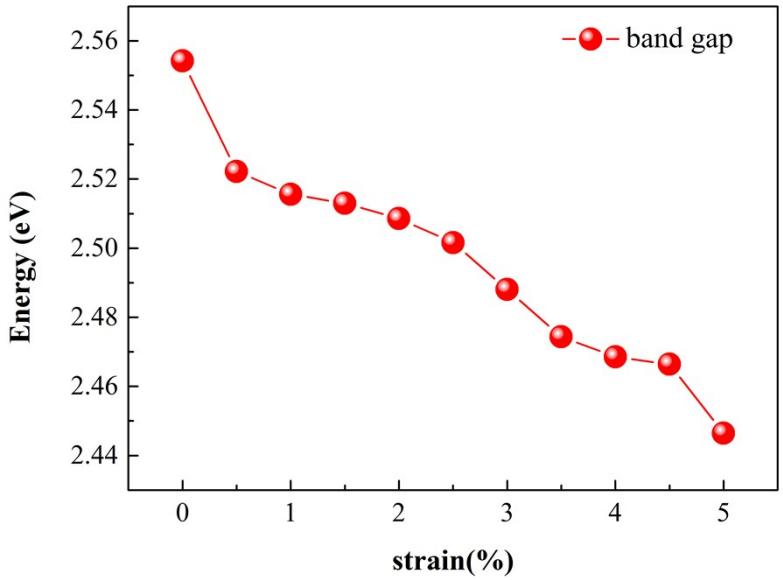

Figure S6. The calculated band gaps of BA_2PbBr_4 under various biaxial tensile strains along *ab* plane.

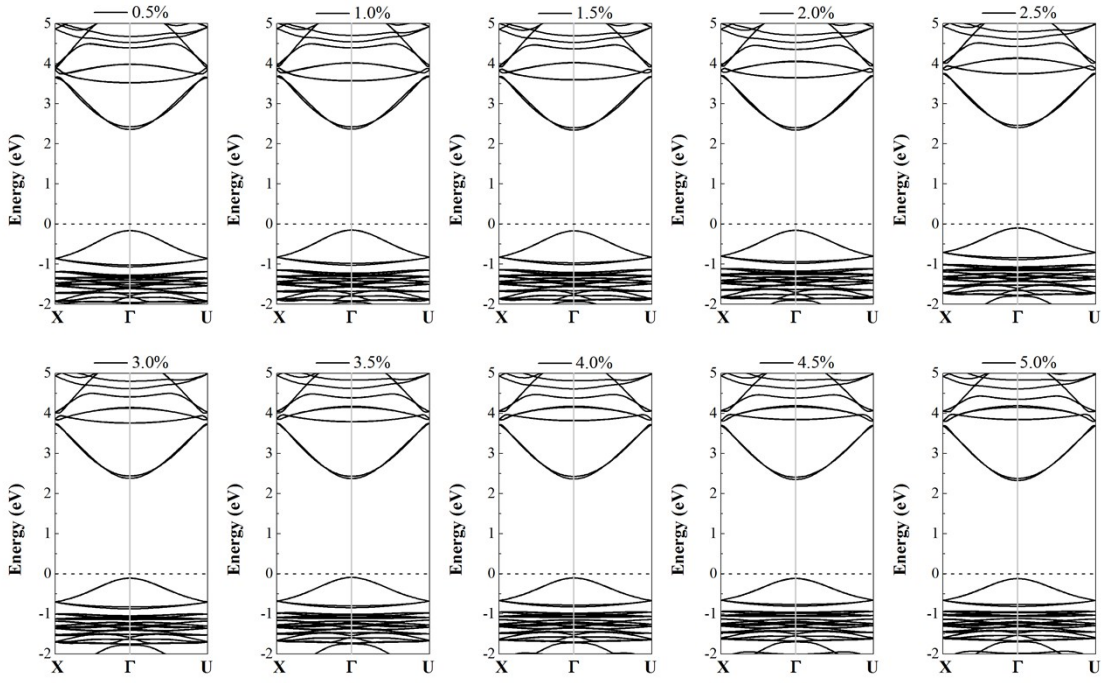

Figure S7. The detailed band structures of BA_2PbBr_4 under various biaxial tensile strains along *ab* plane.

Table S3. Calculated effective mass m^* (unit: m_e), deformation potential constant $|E_1|$(unit: eV), elastic constant C (unit: GPa), and carrier mobility μ (unit: $cm^2\ V^{-1}s^{-1}$) for BA_2PbBr_4 along the *a* (*Γ*-*X*) and *b* (*Γ*-*U*) directions under various strains.

Strain	Holes		Electrons		C	$\|E_1\|$	Holes		Electrons	
(%)	m_a^*	m_b^*	m_a^*	m_b^*			μ_a	μ_b	μ_a	μ_b
0	0.300	0.325	0.224	0.244	69.44	13.54	46.94	38.43	97.44	78.68
0.5	0.298	0.325	0.220	0.240	69.60	14.49	41.76	33.62	89.17	71.74
1	0.301	0.33	0.219	0.240	69.22	15.06	37.50	29.79	83.04	66.05
1.5	0.309	0.338	0.221	0.242	68.74	15.97	31.02	24.79	71.71	57.15
2	0.313	0.344	0.220	0.241	68.38	16.87	26.78	21.15	64.66	51.48
2.5	0.326	0.356	0.224	0.245	67.93	17.70	21.83	17.52	55.78	44.58
3	0.327	0.358	0.222	0.244	67.59	18.24	20.29	16.18	53.44	42.19
3.5	0.324	0.357	0.218	0.240	67.11	18.60	19.84	15.56	53.41	42.00
4	0.337	0.371	0.221	0.244	66.49	18.92	17.21	13.53	49.42	38.58
4.5	0.349	0.385	0.223	0.246	66.11	19.28	15.10	11.81	46.27	36.20
5	0.342	0.378	0.220	0.243	65.71	19.54	15.37	11.97	46.32	36.13

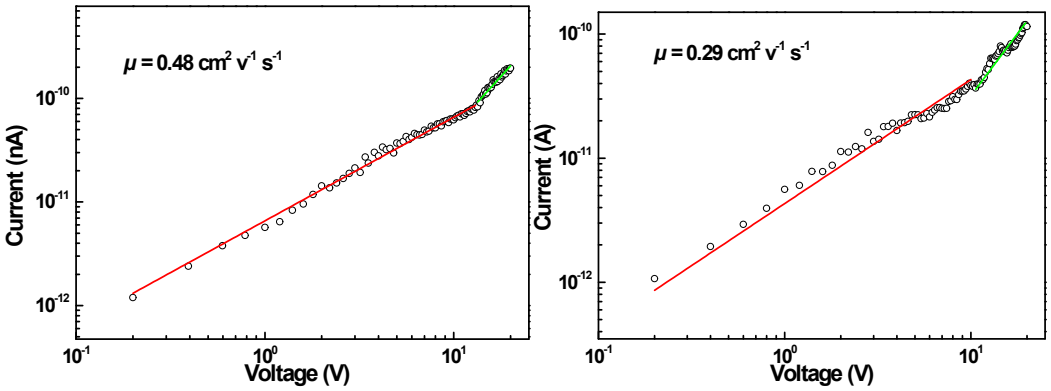

Figure S8. Current-voltage curves for samples with and without strain (0.6%), respectively. Linear and quadratic fitting are applied according to the space charge-limited current (SCLC) model.

Note II. Characterization of responsivity (*R*) and external quantum efficiency (EQE) of the device.

R is defined as the ratio of total photocurrent to the radiation flux, which can be calculated by[2]:

$$R=(I_p - I_d)/(A \cdot P) \quad (3)$$

where I_p and I_d are currents with and without illumination, A is the active area of the device, and P is the incident radiation flux density. EQE is calculated by[3]

$$\mathrm{EQE}=R \cdot hc/e\lambda \quad (4)$$

where h is Planck constant, c is the velocity of light, e is the electronic charge, and λ is the wavelength of the incident light. The responsivity (R) and external quantum efficiency (EQE) of BA_2PbBr_4 were calculated, as shown in **Figure S9**.

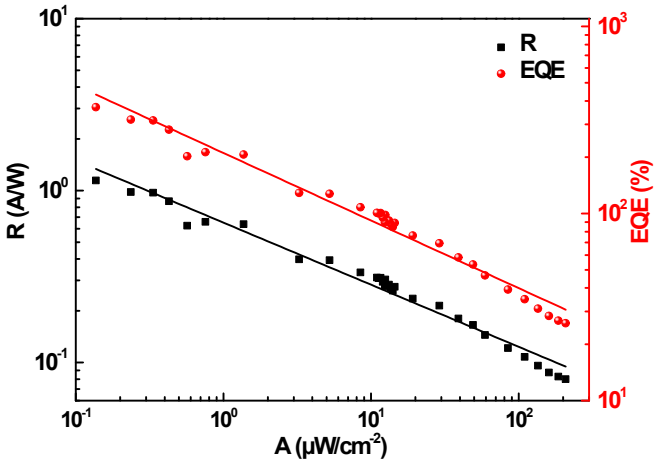

Figure S9. Light intensity-dependent responsivity and external quantum efficiency of the device.

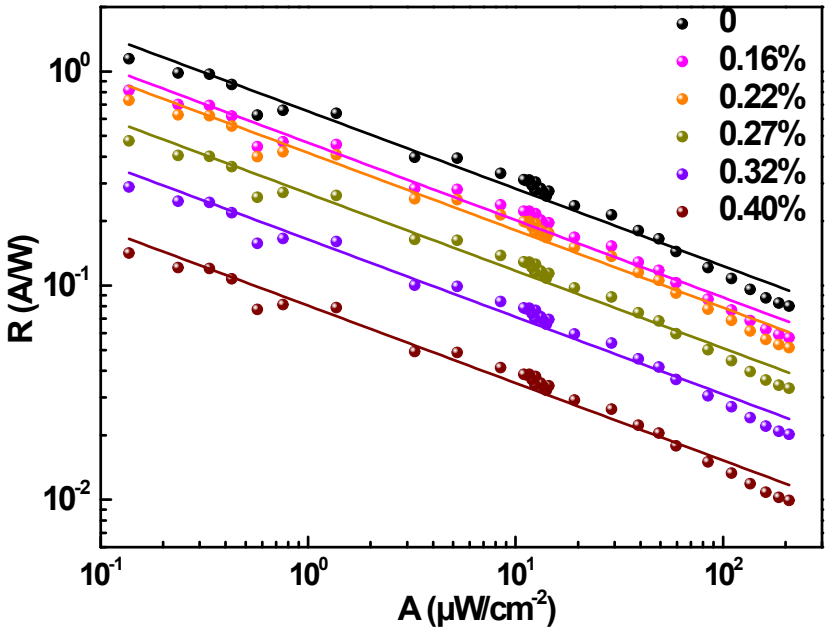

Figure S10. The effect of strain on responsivity of the device.

References:

1 S.-i. Nakamura, *J. Struct. Eng.* **2002**, *128*, 1169.

2 X. Gong, M. Tong, Y. Xia, W. Cai, J. S. Moon, Y. Cao, G. Yu, C.-L. Shieh, B. Nilsson, A. J. Heeger, *Science* **2009**, *325*, 1665.

3 Z. Lian, Q. Yan, Q. Lv, Y. Wang, L. Liu, L. Zhang, S. Pan, Q. Li, L. Wang, J. L. Sun, *Sci. Rep*. **2015**, *5*, 16563.